Journal of
Materials Chemistry A

Accepted Manuscript

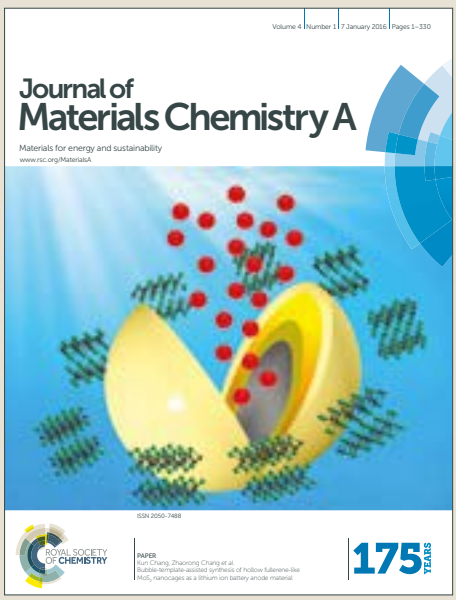

ROYAL SOCIETY OF CHEMISTRY

rsc.li/materials-a

View Article Online
DOI: 10.1039/C8TA00533H

Journal Name

ARTICLE

Ionic liquids as an efficient media assisted mechanochemical synthesis of α-AlH_3 nano-composite

Received 00th January 20xx,
Accepted 00th January 20xx

DOI: 10.1039/x0xx00000x

www.rsc.org/

C. W. Duan[a]*, L. X. Hu[b] and J. L. Ma[c]

Aluminum hydride (AlH_3) is one of the most promising hydrogen storage materials that has a high theoretical hydrogen storage capacity (10.08 wt. %) and relatively low dehydriding temperature (100-200 °C). In this work, we present a cost-effective route to synthesize α-AlH_3 nano-composite by using cheaper metal hydrides and aluminum chloride as starting reagents and to achieve liquid state reactive milling. The LiH/$AlCl_3$ and MgH_2/$AlCl_3$ reaction systems were systemically explored. The phase identification of the obtained products was carried out by XRD and the morphology observed by TEM characterization. It was found that the α-AlH_3 nano-composite can be successfully synthesized by reactive milling of commercial $AlCl_3$ and LiH in a neutral ionic liquid ([2-Eim] OAc). Based on XRD analysis and TEM observation, an average grain size of 56 nm can be obtained by the proposed mechanochemical process. By setting the isothermal dehydrogenation temperature between 80 and 160°C, the as-synthesized α-AlH_3 nano-composite exhibits an advantage in hydrogen desorption capacity and has fast dehydriding kinetics. The hydrogen desorption content of 9.93 wt. % has been achieved at 160 °C, which indicates the potential utilization of the prepared nanocomposite in hydrogen storage applications.

Introduction

An extensive amount of research has been focused on developing a viable, safe and efficient technique for hydrogen storage. Most importantly, various hydrogen storage materials, such as the light metal hydride and their complexes, have been extensively explored over the recent years.[1, 2] Among these materials, aluminium hydride (AlH_3) is one of the most promising candidates due to its high theoretical hydrogen storage capacity (10.08 wt. %) and low decomposition temperature (100-200 ℃).[3-8] Compared to other metal hydride or hydrogen storage materials, AlH_3 is an ideal candidate for a wide array of applications, such as solid rocket propellant and hydrogen-fuel cells.[9-11] Hence, several research groups have investigated the synthesis methods and hydrogen-storage performance of AlH_3 polymorphs.[4, 5, 12-16]

In 1969, Turley and Rinn, firstly, confirmed the crystal structure of α-AlH_3 phase, which crystallizes in a trigonal space group with a hexagonal unit cell.[12] Afterwards, other structural variations of AlH_3 polymorphs (α', β, γ, δ, ε, ζ, orthorhombic Cmcm and cubic $F\overline{3}dm$) were reported by various research groups.[13-16] Among these polymorphs, the α-AlH_3 is recognized as the most stable and, consequently, the most investigated phase. The α-AlH_3 is stable at room temperature, whereas thermodynamically at a higher temperature (150 °C) with an equilibrium decomposition pressure of 10 kbar.[14] Recently, the α-polymorph, has an interatomic Al-H distance that is between that expected for ionic and covalent bonding and therefore has become one of the most researched binary metal hydrides.[12-14] Additionally, the dehydriding capacity and temperature of α-AlH_3 are well above the threshold, set by US Department of Energy (DOE) 2015. The target hydrogen storage requirement of 9 wt. % can also be achieved by controlling the particle size or hybridizing with other metal hydrides, such as LiH and MgH_2.[4, 5]

Developing cost-effective and efficient synthesis approaches for α-AlH_3 remain key issues and limit the practical utilization of this material. Apart from the structural investigations, Brower et al. have synthesized the non-solvated AlH_3 through an organometallic synthesis route in 1967.[17] By adding $LiAlH_4$ and $AlCl_3$ into the ether and heating the resulting $AlH_3 \cdot nEt_2O$ at 65 ℃ for 6.5 h under vacuum, the α-AlH_3 can be preferentially formed according to the Eqn. (1).

$$3LiAlH_{4(sln)}+AlCl_{3\,(sln)}+4nEt_2O \rightarrow 4AlH_3 \cdot nEt_2O_{(sln)}+3LiCl\downarrow \quad (1)$$

It was later discovered by Bulychev et al. that the α-AlH_3 could be directly synthesized by use of Lewis and a Bronsted acid as reagents and crystallizing from diethyl ether-benzene solutions, the reactions are expressed in Eqns. (2) and (3).[18, 19] However, the abovementioned method for α-AlH_3 synthesis is highly sensitive to the temperature and time and not suitable for large-scale AlH_3 production.

$$6MAlH_{4(s)}+7Al_2Br_{6\,(sln)} \rightarrow 8AlH_3\downarrow+6MAl_2Br_7 \quad (2)$$

$$2LiAlH_4+H_2SO_4 \rightarrow 2AlH_3+Li_2SO_4+H_2 \quad (3)$$

It has been reported that the mechanochemical synthesis process is under the umbrella of green chemistry and is a sustainable method to synthesize metal hydrides due to favorable solid-state reactions during ball milling. For instance, Kim et al. have reported that the nanocrystalline $Mg(AlH_4)_2$ (~ 18 nm) can be synthesized by the mechanochemically activated reaction between

[a] Address here.
[b] Address here.
[c] Address here.
† Footnotes relating to the title and/or authors should appear here.
Electronic Supplementary Information (ESI) available: [details of any supplementary information available should be included here]. See DOI: 10.1039/x0xx00000x

View Article Online
DOI: 10.1039/C8TA00533H

$NaAlH_4$ and $MgCl_2$ without the use of any solvents.[20] It has been reported by Møller et al. that the $NaBH_4$ and $Ca(AlH_4)_2$ can be formed by mechanochemical treatment of $NaAlH_4$ and $Ca(BH_4)_2$ mixtures.[21] Birke et al. have suggested that the mechanochemical method offers distinct economic benefits, such as a low energy of consumption and utilization of cost-effective reagents.[22] Moreover, it has been demonstrated by Tigineh et al. that the mechanochemical process is solvent-free and consumes less energy, which makes them greener and sustainable than the conventional solution-based processes.[23] Furthermore, Park et al. have demonstrated that the dry-nature of the mechanochemical method makes it compatible with the current push to green-chemistry alternatives by avoiding the use of expensive and hazardous organic solvents during the synthesis process.[24] Thus, this method is considered as a powerful tool to employ solid-state reactions for metal hydrides synthesis. Based on the drawbacks of above-mentioned wet chemical techniques, Brinks et al. have employed a mechanochemical method to synthesize AlH_3.[14] It has been demonstrated that the AlH_3/LiCl composite can be synthesized by a mechanically assisted reaction, between $LiAlH_4$ and $AlCl_3$ at room temperature and 77 K.[14] The reaction can be described by Eqn. (4).

$$3LiAlH_{4(s)}+AlCl_{3(s)}\rightarrow 4AlH_3+3LiCl \quad (4)$$

Lately, Sartori et al. have discovered that the yield of AlH_3 can be increased to 49.9 mol % by using $NaAlH_4$, as a reagent, and FeF_3, as a catalyst.[25] It has been demonstrated by Paskevicius et al.[26] that the AlH_3 can be formed via a mechanochemical reaction of $LiAlH_4$ and $AlCl_3$ at lower or room temperature, which results in several polymorphs (α-, α'-, and γ -AlH_3) with the crystalline size of 15 – 17 nm. Nevertheless, this work was solely focused on the mechanochemical synthesis of AlH_3 composite rather than aiming for a specific crystal structure. The as-milled AlH_3, with some variations in its crystal structures, ultimately leads to the complexity of the extraction. This solid state mechanochemical method has also been adopted for use by other researchers to produce nano-sized α-AlH_3 composite.[27-31] Because of its widespread use, it is evident that mechanochemical method is a valid and well-established method for the synthesis of nano-sized α-AlH_3 composite. However, it has been reported that the metallic Al forms during the room temperature ball milling, which can be partially attributed to the heterogeneity of solid-state reaction and leads to the decomposition of AlH_3. Though the cryo-milling process has the potential to prevent the AlH_3 from dehydriding, the much lower temperature also raises technical challenges on large-scale production of α-AlH_3.

Ionic liquids (ILs) are considered as promising environment-friendly solvents in organic synthesis and offer distinct advantages, such as non-flammability, low volatility, low toxicity and high thermal and chemical stability.[32, 33] ILs are also extremely important because they can be used as a solvent in catalyst-free reactions. To date, series of catalyst-free reactions are employed and completed in ILs due to the ease of the experimental procedure, low cost and eco-friendly process.[34, 35] Due to the advantages offered by ILs over traditional approaches, we aimed to employ ILs solvent to synthesize α-AlH_3. In order to stabilize the obtained α-AlH_3 during the mechanochemical process, the selection of ionic liquid is critical. Compared with acidic ionic liquids, the neutral ILs are more suitable for synthesis of α-AlH_3 because the protonic acid is eliminated and the mechanochemical reaction can be performed at a lower temperature under neutral conditions. To overcome the heterogeneity of the solid state reaction and stabilize the synthesized α-AlH_3 during the mechanochemical process, the [2-Eim] OAc ionic liquid has been induced as the efficient neutral media.

Enormous interest in α-AlH_3 has urged us to explore green and straightforward mechanochemical route. Herein, we propose a sustainable and green synthesis process for α-AlH_3 by employing liquid state reaction milling process and using cheap metal hydrides and aluminum chloride as reagents. In the present investigation, the LiH/$AlCl_3$ and MgH_2/$AlCl_3$ are considered as the reaction system, separately. The [2-Eim] OAc (2-ethyl imidazolium acetate) is used as an efficient neutral media ionic liquid for α-AlH_3 synthesis.

The proposed synthesis approach is more sustainable, convenient and eco-friendly than the previously reported methods. Furthermore, the effective utilization of cost-efficient raw materials, such as LiH and $AlCl_3$, the catalyst-free synthesis and low energy consumption indicate the distinct advantages of the applied synthesis process. For instance, the LiH utilized in this study is cheaper than $LiAlH_4$. As a conventional raw materials, LiH was always be used for producing $LiAlH_4$. In contrast, the conventional method for synthesizing AlH_3 is conducted in ether solvent using $LiAlH_4$ and $AlCl_3$ as reagents and the whole process is not sustainable and green. In addition, the MgH_2 was prepared by milling cheap Mg powder under lower hydrogen pressure, which is a green process with high energy efficiency and does not require hazardous solvents.[36] The synthesis of α-AlH_3 nano-composite was carried out by milling $AlCl_3$ and LiH powders in hydrogen, without any catalyst. Moreover, the utilized [2-Eim] OAc ionic liquid is eco-friendly and facilitates the stabilization of AlH_3. The adopted lower ball-to-powder ratio results in less energy consumption, which makes this process more sustainable. Furthermore, Paskevicius et al. have demonstrated the synthesis of several polymorphs of AlH_3 (α-, α'-, β-, and γ -AlH_3) via a chemical reaction between $LiAlH_4$ and $AlCl_3$ at 77 K and RT.[26] However, in our proposed method, the α-AlH_3 phase can be directly obtained during ball milling, which facilitates of the following extraction.

As outlined by thermodynamic processes, the Gibbs free energy change for the reactions between LiH and $AlCl_3$, MgH_2 and $AlCl_3$ are calculated from the Eqns (5) and (6). The Gibbs free energy changes for the reactions from 273K to 373K are both less than 0 kJ/mol, as shown in Fig. S1, which indicates that these reactions can take place at room temperature. However, according to the reaction kinetics, the feasibility of the mechanochemical reaction has to be experimentally demonstrated by ball milling.

$$3LiH+AlCl_3\rightarrow 3LiCl+AlH_3 \quad (5)$$

$$3MgH_2+2AlCl_3\rightarrow 2AlH_3+3MgCl_2 \quad (6)$$

Experimental

The nanocrystalline MgH_2 (self-made, 99%), LiH (Sigma Aldrich, 97%), $AlCl_3$ (Sigma Aldrich, 99%) and [2-Eim] OAc were employed as starting reagents and solvent to synthesize α-AlH_3 composite. The nanocrystalline MgH_2 powder was prepared by mechanochemical reaction between Mg powder and H_2, as reported previously.[36] The

View Article Online
DOI: 10.1039/C8TA00533H

LiH, $AlCl_3$ and [2-Eim] OAc were used without any further purification (refer to ESI, Fig. S2 and S3). Due to the high sensitivity of the reagents and as-milled products to moisture content, all manipulations including charging and discharging of vials throughout experiments were conducted in an Ar-filled gloves box, with oxygen and water content of less than 5 and 2 ppm, respectively.

For a typical mechanochemical reaction, the reagents, LiH/$AlCl_3$ and MgH_2/$AlCl_3$ as well as [2-Eim] OAc were weighed and mixed in the various molar ratios(3:1, 4:1, 6:1, 9:1 and 3:2) and transferred to a high-pressure planetary type ball milling machine (QM-SP4), with 500 cm^3 ball milling chamber. The reaction mixture was sealed into the container under Ar atmosphere in gloves box. The argon atmosphere was purged twice, with zero grade H_2, before the container was finally pressurized to 5 MPa H_2 pressure. During the mechanochemical reaction, the ball to powder mass ratio were 20, 40 and 60:1 and high-energy milling was carried out for various time intervals at 200 rpm. The abovementioned ball to powder ratio is lower than the study carried out by Sartori et al., where the ball to powder ratio was 200:1.[25,30] The lower ball to powder ratio results in less energy consumption, which makes it more sustainable. To keep the average temperature in the vial as close to room temperature as possible, the milling sequence was altered every twenty minutes, with an intermittent pause of ten minutes. After completion of the mechanochemical reaction, the as-milled product was filtered and distilled in a vacuum. The crude ionic liquid [2-Eim] OAc was washed with diethyl ether and dried in a vacuum oven at 80 °C for further experiments.

To study the dehydriding properties of as-milled samples, dehydriding measurements were carried out on a home-made special vacuum apparatus. The as-milled powder was loaded into a stainless steel holder. The evacuated volume inside the apparatus can reach up to 1×10^{-2} Pa, at the initial stages of isothermal desorption measurements. In order to investigate the dehydriding kinetics of composite systemically, the as-milled samples were powdered at different temperatures of 80, 120, 140 and 160 °C. The time required for the full dehydriding reaction was fixed at 6.5 $\times$ 10^3 s. The amount of hydrogen decomposed from the composite was measured and calculated in terms of the vial vacuum change. Based on the H_2 pressure change, the ideal gas equation, as well as the stoichiometric weight of AlH_3 calculated by the chemical reaction, the content of AlH_3 in nanocomposite, could be obtained. The dehydriding curves of the AlH_3 nano-composite were obtained. The differential thermal analysis measurements were performed by using a TG-DSC METTLER TOLEDO instruments. The samples were handled and transferred to the instrument in T-zero pans and heated from 50 to 280 °C, by using different heating rates. In order to prevent the air exposure, the composite was sealed in an aluminum crucible.

The X-ray powder diffraction (XRD) analysis of the as-milled products was performed by using a diffractometer, equipped with a graphite monochromator and rotating anode tube, operating with Cu Kα radiation source at 45 kV and 40 mA. The XRD patterns were collected by using step scanning mode, at a rate of 0.5°/min, in the 2θ range of 10 - 90°. The average grain size of the α-AlH_3 phase (G) was obtained by using Scherrer formula according to the following equation:

$$D = \frac{k\lambda}{\beta cos\ \theta} \quad (7)$$

Where D represents the average grain size, k is a constant with a value of 0.89, λ corresponds to the applied X-ray wavelength ($\lambda_{Cu\text{-}K\alpha}$ = 1.54 Å), β is defined as the half-width after subtracting for the instrumental broadening and θ corresponds to the diffraction angle of the diffraction peak.

The solid-state NMR experiments were carried out at 14.1 T magnet on a Bruker Avance NMR spectrometer, equipped with a magic angle spinning probe head for rotors of 2.5 mm diameter. Due to the air and moisture sensitivity of the materials used in experiments, all the solid samples were packed into a 2.5 mm ZrO_2 rotor in a gloves box under argon atmosphere. To maximize quantitative accuracy, the direct polarization spectra were spun under 20 KHz to identify the resonances and spinning sidebands. The chemical shift scale was referenced externally with potassium alum to -0.033 ppm as a secondary reference, and recycle delay for ^{27}Al was set to 3 sec. The transmission electron microscopy (TEM) analysis was carried out on the JEOL JEM2011 apparatus. For TEM observations, the powders were loaded onto the carbon support films, with 200 mesh copper grids. It should be noted that the as-milled products, mixed with [2-Eim] OAc, were filtrated and dried in a vacuum oven before dehydriding, TEM and NMR measurements.

Results and discussion

Selection of mechanochemical reaction reagents

The solid-state synthesis of alane via mechanochemical reaction of LiH or MgH_2 precursors with $AlCl_3$ has been demonstrated as an efficient and green method of producing adduct-free AlH_3 in large quantities.[5, 26, 31, 37-40] Hlova et al. [31] have found that the amorphous AlH_3 can be formed by milling LiH and $AlCl_3$ at room temperature. Moreover, the successful synthesis of γ-AlH_3/$MgCl_2$ nano-composite has been demonstrated by solid-state milling of nanocrystalline MgH_2 and $AlCl_3$, which is also a cost-effective method to obtain γ-AlH_3 nano-composite.[37-40] However, the formation of α phase has not been demonstrated by above reports mentioned. Based on the previous investigation, the MgH_2/$AlCl_3$ and LiH/$AlCl_3$ as the reaction systems are employed and introduced into ILs to synthesize α-AlH_3. Fig. 1 shows the XRD patterns of the MgH_2 and $AlCl_3$, with a ratio of 3:2, milled in [2-Eim] OAc for different time intervals. As suggested by the XRD patterns, an amorphous-like background between 10° to 20° can ascribe to the [2-Eim] OAc, which was used as a solvent in the mechanochemical synthesis of AlH_3. Only the diffraction peaks, corresponding to $Mg(AlH_4)_2$ and $MgCl_2$ were found at milling time = 1 hrs, which result suggests that the following reaction has occurred initially (Eqn.8). This is mainly due to the higher chemical reactivity of nanocrystalline MgH_2 (Fig. S2). It also indicates that the formation of $Mg(AlH_4)_2$ requires lower activation energy, as compared to the AlH_3, synthesized in [2-Eim] OAc. Even with prolonged reaction times, the XRD patterns did not indicate the presence of AlH_3 traces (Fig. 1 b and c). However, the $Mg(AlH_4)_2$ was still found to be a major phase in the as-milled product. This phenomenon is in good agreement with the previously published report,[41] where $Mg(AlH_4)_2$ was obtained by ball milling MgH_2 and $AlCl_3$ in a molar ratio of 3:2 at low temperature. Moreover, the grain

View Article Online
DOI: 10.1039/C8TA00533H

size of $Mg(AlH_4)_2$, obtained after 2.5h milling, reduced to 32 nm. It can be concluded that $Mg(AlH_4)_2$ phase has transformed into a nano-crystallite form. Based on above analysis, it can be concluded that it is difficult to obtain AlH_3 by mechanochemical reaction of MgH_2 with $AlCl_3$ in [2-Eim] OAc. Hence, LiH was used to replace MgH_2.

$$4MgH_2+2AlCl_3 \rightarrow 2AlH_3+MgH_2+3MgCl_2 \rightarrow Mg(AlH_4)_2+3MgCl_2 \quad (8)$$

Fig.2 shows the XRD patterns of fresh samples, prepared by ball milling a mixture of LiH and $AlCl_3$ (3:1) in [2-Eim] OAc for different time intervals. After milling for 1 h, the diffraction peaks corresponding to the starting reagents were still observed, which indicates that the AlH_3 cannot be synthesized under this condition. When milling time was increased to 2 h, the observed diffraction peaks correspond to the starting reagents (LiH and $AlCl_3$) and $LiAlH_4$. Even at a milling time of 2.5 h, the formation of AlH_3 was not observed (Fig. 2c). However, an alternate crystalline phase, $LiAlH_4$, has formed during the ball milling. It can be concluded that the LiH and $AlCl_3$ have reacted to form $LiAlH_4$, instead of AlH_3. It is worth noting that molar ratio in these experiments was fixed at 3:1. It has been reported that AlH_3 can be formed by mechanochemical reaction of Li precursors ($LiAlH_4$ and LiH) if the mole ratio of reagent is chosen properly.[5, 38] Therefore, we aimed to optimize the synthesis process by varying the molar ratios, ball to powder ratio, the mill shaft rotation speed and milling time to obtain α-AlH_3 by mechanochemical process.

Determination of mechanochemical reaction conditions

Based on above analysis, when a stoichiometric 3:1 molar mixture was used to start the reaction, the $LiAlH_4$ is formed during the ball milling. The effect of molar ratio (4:1, 6:1 and 9:1) was studied by changing the relative amount of LiH and $AlCl_3$. Fig. 3 displays the XRD patterns of LiH with various ratio of $AlCl_3$ milled for 1h, with the ball to powder mass ratio of 40:1. When the ratio was fixed at 4:1, the results were similar to those prepared by milling the LiH/$AlCl_3$ mixture with a ratio of 3:1, but it appeared that the reaction process had been accelerated. Complete reaction of LiH and $AlCl_3$ with the formation of $LiAlH_4$ was achieved on milling the mixture for 1h. Therefore, the ball-to-powder ratio is regarded as an important parameter during the mechanochemical process, which can effectively enhance the chemical reactivity between the reagents. The complexity and uniqueness of the mechanochemical reaction, with respect to the precursors, indicates that the above result may not be fully applicable to the LiH-$AlCl_3$ system, which motivated us to carry out an in-depth investigation on the ratio of reagents. When initial reactions between LiH and $AlCl_3$ were performed for different molar ratios (4:1 to 6:1), it can be readily observed that the $LiAlH_4$, Li_3AlH_6 and LiCl were major products (Fig. 3). The presence of $LiAlH_4$ and Li_3AlH_6, after 1 h of ball milling, can be explained by the following reaction (Eqn 9).[42] As shown in Fig. 3, for the starting mixture of 9:1, only Li_3AlH_6, LiCl and unreacted LiH diffraction peaks were observed. Thus, it can be concluded that the excess of Li hydride source leads to the formation of Li_3AlH_6. This observation is in good agreement with our previous investigation, where Li_3AlH_6 was observed as the final product.[38]

$$2LiH + LiAlH_4 \rightarrow Li_3AlH_6 \quad (9)$$

Hlova et al. [31] have reported a transformation pathway for synthesizing AlH_3, where the solid-state mechanochemical reaction can be controlled by step-wise addition of $AlCl_3$ to the initial reaction mixture. In order to obtain AlH_3 by mechanochemical reaction of LiH with $AlCl_3$, the same pathway was adopted in our present investigation. During the second stage of the reaction process, 1/3 molar equivalents of $AlCl_3$ were added to the products obtained from the 4:1 reaction of LiH and $AlCl_3$ ($LiAlH_4$, LiCl at τBM = 60 min) to reach the desired ratio of 3:1. Fig. 4 demonstrates the XRD patterns of the $LiAlH_4$/LiCl composite with a mixture of $AlCl_3$ milled for 20, 40, 60 and 80 min, and with the same ball to powder mass ratio as previously mentioned. It can be seen from that the diffraction peaks corresponding to the unreacted $AlCl_3$, along with the previously present LiCl and $LiAlH_4$, were observed after 20 minutes of milling. This could be ascribed to the incomplete reaction of $LiAlH_4$ and $AlCl_3$. It is noted that a new set of diffraction peaks appeared at 28-29° and 48°, which could be unambiguously assigned to $LiAlCl_4$. This result is in good agreement with the previously published literature.[43] Upon further milling for 60 min, the peaks of $LiAlH_4$, $LiAlCl_4$ and $AlCl_3$ phase disappeared from the XRD patterns and the complete mechanochemical reaction has been achieved. Meanwhile, there was a change in the mixtures for the as-milled samples, reacted between 20 and 60 min, as compared to the starting precursors. The intensities of the peaks between 10° and 20° gradually increased, indicating that an amorphous intermediate has formed. According to the latest report,[31] it has been demonstrated that LiH/$AlCl_3$ reagents may undergo an amorphization stage before the final AlH_3 phase formation. Thus, with the increased milling time, the crystallization and stabilization of the intermediate phase have been achieved (Fig. 4). From XRD pattern of the as-milled samples, milled for 60 min, it is obvious that the crystallization of α, γ-AlH_3 was achieved. This phenomenon also demonstrates that the formation of α and γ phases is more favorable than other less stable phases. With prolonged reaction time, it can be concluded that only α-AlH_3 phase was eventually formed and transformed into a nano-crystallite form. The crystallite size, calculated from XRD patterns, demonstrated that the average crystallite size of the α-AlH_3 phase obtained by 80 min milling could reach 128 nm. From the XRD patterns, it can be observed that no impurity phase was present in the final as-milled products. This may be attributed to the stabilization of the [2-Eim] OAc, which can not react with a product, such as AlH_3 or LiCl during the milling process.

In order to obtain α-AlH_3 composite as the final product in a short milling time, the as-milled $LiAlH_4$/LiCl mixture was milled with a ratio of 60:1 for various time intervals. When milled for 20 min, the intensity of the peaks, assigned to $LiAlH_4$ and $AlCl_3$, decreased significantly, suggesting that the decrement of reagents and the increment of the mechanochemical reaction extent (Fig. 5). In addition, it can be seen that no diffraction peaks of $LiAlH_4$ and $AlCl_3$ were detected in the sample milled for 40 min. It appeared from Fig. 5 that the complete reaction of $LiAlH_4$ and $AlCl_3$, with the formation of α-AlH_3, has been achieved in final milling stage. It can be concluded that the ball-to-powder ratio is an important parameter, which effectively increases the reaction kinetics and decreases the reaction time to form α-AlH_3 nano-composite. When the milling time was increased to 60 min, the final crystallite size of α-AlH_3 reduced to 56 nm. In short, the adopted mechanochemical pathway can be regarded as a green and simple way to synthesize α-AlH_3 nano-composite by step-wise addition of $AlCl_3$ into LiH

View Article Online
DOI: 10.1039/C8TA00533H

reaction system. Furthermore, the elimination of hazardous solvents from the synthesis process is the distinct advantage of this process.

Identification of as-milled powders

To confirm the XRD results and the existence of an amorphous phase in the as-milled product, the sequence of events during the mechanochemical process (stage II) was also monitored by NMR spectroscopy. The as-milled samples during the mechanochemical process were characterized by ^{27}Al DPMAS spectroscopy, which is shown in Fig. 6. It can be seen that a peak centered around -2 ppm was detected in Fig. 6a, which can be ascribed to the presence of $AlCl_3$. This indicates that $AlCl_3$ was not entirely consumed within the first 20 min of milling. The dominant spectral band around 100 ppm (Fig. 6a) represents the resulting four-coordinated (Al^{IV}) species. The Al^{VI} signal consists of two superimposed central transition powder patterns ascribed to $LiAlH_4$ and $LiAlCl_4$. However, the relative contributions of $LiAlH_4$ and $LiAlCl_4$ are difficult to quantify and be resolved in a DPMAS spectrum due to severe spectral overlap. This assignment has been elucidated in Hlova's study, based on the DPMAS spectra of $LiAlH_4$ and $LiAlCl_4$ in neat form.[31] When the milling time was increased to 40 min, the NMR spectrum suggested that $AlCl_3$, $LiAlH_4$ and $LiAlCl_4$ got consumed in the as-milled composite. On the contrary, it consists of a prominent peak, centered around 4-8 ppm, indicating the formation of six-coordinated Al^{VI} species in the composite. It is difficult to find any crystal structure report or NMR data for these hydrogen-substituted aluminum halides. According to Gupta's report,[5] it has been suggested that this intermediate might still contain more than one Al species. Even after milling for 60 min, the DPMAS spectrum was similar to the one observed for 40 min. This result confirms that no peaks indicative of $LiAlCl_4$ or $LiAH_4$ were identified in the spectrum, which suggests the termination of the mechanochemical reaction. However, it can be seen from Fig. 6 that there is a substantial change in the peak of six-coordinated Al^{VI} species. The evolution of the Al^{VI} peak may be attributed to the ensuing phase conversion of intermediates such as Li-Al-H or Al-H into AlH_3 during extended milling. It has previously been demonstrated by Humphries et al. that the resonance bands around 5.9 ppm are indicative of a α-AlH_3 phase.[44, 45] Therefore, this result confirmed the formation of α-AlH_3, as the final product, after 60 min milling.

The transmission electron microscopy (TEM) is uniquely suited to study the phase transition at nano-scale.[46] It has been demonstrated by Nakagawa et al. that the a-AlH_3 can be clearly identified from the selected area electron diffraction (SAED) pattern.[7] Moreover, it has been reported that AlH_3 is stable under the electron beam.[37, 38] Thus, TEM observation and associated SAED patterns were monitored and these results indicate the presence of α-AlH_3 and LiCl phases in as-milled products. It can be seen from Fig. 7 that the crystallization of α-AlH_3 was complete at following the end of the milling stage. Furthermore, Fig. 7a shows that the average grain size of α-AlH_3 was 56 nm after 60 min milling. This result is in good agreement with our previous work, where only α-AlH_3 and LiCl phases were observed in XRD patterns. The typical lattice spacings of 0.323, 0.234 and 0.222 nm correspond to the (012), (104) and (110) planes of α-AlH_3, respectively (Fig. 7b). Moreover, the corresponding SAED patterns (Fig. 7b) indicate the crystalline nature of nanocomposite with (111), (200), (220) and (400) planes of the LiCl. The morphology of α-AlH_3 nanoparticles is similar to the results of TEM investigations carried out by Paskevicius et al.,[26] where the product consists of α-AlH_3 nanoparticles embedded in a LiCl by-product.

De-hydriding property of α-AlH_3 composite

Fig. 8 shows the dehydriding kinetics of the as-milled α-AlH_3 composite at various temperatures and time intervals. It is noteworthy that the dehydriding content is calculated by dividing actual hydrogen content by the stoichiometric AlH_3 weight. As seen from Fig. 8, all the isothermal dehydriding curves present sigmoidal features with introduction, acceleration and decay periods. The results indicate that the rate of dehydrogenation accelerated as the temperature rose to 160 °C. Additionally, from the dehydrogenation curves, it can be conjectured that dehydriding temperature has a remarkable effect on the dehydrogenation reaction of α-AlH_3/LiCl composite, which can be expressed by Eqn. (10).

$$AlH_3 \rightarrow 2Al + 3H_2\uparrow \qquad (10)$$

When the dehydriding temperature was fixed at 80 °C for $2.84*10^3$ s, it can be seen from the Fig. 8a that the hydrogen desorption content of as-milled product reached merely 2.0 wt. %, indicating the partial dehydriding reactions. Although the dehydriding curves exhibited an undesirable property, the as-milled product still has an advantage in dehydriding properties, compared to the much lower hydrogen content of 1.9 wt. % derived from the as-milled AlH_3, which entirely decomposed from room temperature to 200 °C.[5] Furthermore, the value described above, is higher than the 0.48 wt. % hydrogen content of crude α-AlH_3, measured by Graetz. et al.[6, 8, 47] By increasing the reaction temperature to 120 °C, the hydrogen content of α-AlH_3 composite increased rapidly to 7.29 wt. %, suggesting that a large part of AlH_3 decomposed at a higher temperature. Furthermore, 9.93 wt. % of hydrogen desorption could be obtained by heating the reaction mixture at 140 °C for the same time, which implies that the dehydrogenation rate has a direct relationship with the temperature. Afterwards, the as-milled composite was annealed at 160 °C for 860 s and the hydrogen content reached a maxima up to 9.93 wt. %, which is quite close to the theoretical hydrogen storage capacity (10.08 wt. %) of pure AlH_3. It is worth mentioning that the AlH_3, prepared by the organometallic method,[48] can only release 8.0 wt. % of H_2 in the temperature range of 20-160 °C. Although the freshly synthesized nanoscale α-AlH_3 has an enhanced dehydrogenation property, it has been reported by Graetz et al. that the complete decomposition at 138°C can be achieved even within 1800 s.[49] Therefore, it can be concluded that nano-structured α-AlH_3 composite, characterized by much finer grain size, exhibits excellent dehydriding performance.

Though, the dehydriding temperature of the α-AlH_3 nanocomposite is higher than usual and lower dehydriding temperature is favorable in hydrogen storage materials. However, it has been demonstrated by Graetz et al. that the AlH_3 with a dehydriding temperature of 100 to 200 °C can be considered as an ideal candidate for hydrogen storage.[6, 8] Despite the high dehydriding temperature, the AlH_3 is an excellent candidate for hydrogen storage due to its high theoretical hydrogen storage capacity. The dehydriding temperature can be reduced by a number

View Article Online
DOI: 10.1039/C8TA00533H

of approaches. For instance, the effective doping enhances the dehydriding kinetics of AlH_3 and fundamental understanding of the additives' effect is required to optimize the AlH_3 performance. It has been reported that the desorption properties can be improved by the reactive hydride composites between AlH_3 and other compounds, such as $MgCl_2$,[39] MgH_2 [50, 51] and $LiBH_4$.[52] Ti is also considered as an effective catalyst for enhancing the desorption properties of AlH_3. The significant enhancement in dehydriding kinetics was observed by adding $TiCl_3$ in the solution, during the AlH_3 synthesis.[53] Moreover, it has been reported by Sandrock et al. that the onset decomposition temperature of AlH_3 can be reduced to below 100 °C by LiH addition.[54] According to the Sandrock's report, 2 mol % of LiH was added to the α-AlH_3/LiCl nanocomposite. It can be observed, from Fig. S4, that when the dehydriding temperature was fixed at 80 °C, the time to attain complete decomposition decreased rapidly. Compared with the α-AlH_3/LiCl nano-composite without adding LiH, the AlH_3 in the presence of LiH has shown enhanced dehydriding performance, with 9.86 wt. % of hydrogen content at 80 °C for 3400 s. This observation is consistent with the Sandrock's report,[54] which has shown that the decomposition kinetics of AlH_3 can be accelerated by LiH doping. We suggest that if LiCl can be fully separated from this composite, the obtained pure AlH_3 doped with LiH will have an excellent dehydriding property and can be used as an onboard hydrogen storage material.

In order to get a deep insight into the dehydriding process of the α-AlH_3/LiCl nano-composite, further evidence was obtained by the DSC curves. Fig. 9 presents the DSC curves of the as-milled α-AlH_3 composite at several heating rates. It can be clearly observed that as-milled α-AlH_3 curves contain only one endothermic peak, at an elevated temperature of 50 – 280 °C, corresponding to the α-AlH_3 decomposition and consistent with published literature.[51, 55, 56] Liu et al. have found that the endothermic peak between 80 and 190 °C can be assigned to the dehydriding reaction of the α phase.[55, 56] For instance, for as-milled α-AlH_3 composite with a heating rate ranging from 15 to 3 °C/min, the corresponding absolute temperature reduced from 157.4 °C to 121.6 °C. To further explore the dehydrogenation property of α-AlH_3 nano-composite, the dehydriding kinetics of α-AlH_3/LiCl were investigated by Kissinger's method (Eq. 11), particularly in terms of apparent activation energy (E_a).

$$\ln(c/T_p^2) = -(E_a/RT_p)+A \quad (11)$$

Where c corresponds to the heating rate, T_p represents the absolute temperature, corresponding to the maximum desorption rate, R refers to the universal gas constant and A is a constant. Fig. 9b shows the activation energy of the dehydriding reaction based on parameters obtained from the DSC measurements (Fig. 9a). The activation energy of dehydriding reaction of as-milled α-AlH_3 is 56.8 KJ/mol, a value much lower than those calculated by Herley et al.[57] who have reported the activation energy of 157 KJ/mol for α-AlH_3 with an average particle size of 50 μm. This value is also lower than result reported by Cao et al.,[58] who found that the apparent activation energy of the first dehydrogenation step of $Y(AlH_4)_3$ is 92.1 KJ/mol. Gabis et al.[59] have demonstrated that by grain size refinement, the activation energy for dehydriding reaction of α-AlH_3, can be reduced to 104 KJ/mol. Therefore, the as-milled α-AlH_3 composite had lower activation energy and exhibited faster dehydriding kinetics than as-prepared α-AlH_3 with larger grain size.

Conclusions

In this paper, a benign and cost-effective route was developed to synthesize α-AlH_3 (alane) at room temperature by employing liquid state reactive milling. The proposed mechanochemical method was proved to be green and convenient synthesis route for the α-AlH_3 composite. By selecting the appropriate reagents and optimizing the relative amount and milling parameters, the α-AlH_3 nano-composite could be synthesized by reactive milling of commercial $AlCl_3$ and LiH in [2-Eim] OAc. Most importantly, the reaction pathway was controlled by step-wise addition of $AlCl_3$ into the reaction system and determined as the most critical parameter in the mechanochemical synthesis of α-AlH_3/LiCl nano-composite. In the second stage, when 1/3 molar equivalent of $AlCl_3$ was added to the milling product (the product obtained from ball milling of LiH and $AlCl_3$ for 60 min), the reactional system undergoes an amorphization stage before the final product, with the desired product α-AlH_3/LiCl being formed. The average crystallite size of α-AlH_3, embedded with LiCl obtained by mechanochemical reaction in [2-Eim] OAc for 2 h, reached to 56 nm. In particular, the crude ionic liquid [2-Eim] OAc can be recycled for the secondary use. In comparison with the pure α-AlH_3, the as-milled α-AlH_3 nano-composite exhibited an advantage in hydrogen desorption capacity, particularly in the de-hydriding kinetics, with desirable hydrogen desorption amount of 9.93 wt. % within 860 s at 160 °C. Thus, the proposed mechanochemical method offers a green and sustainable room-temperature approach for the large-scale production of α-AlH_3 nano-composite. The unsolvated alane can be successfully applied as a promising material for hydrogen storage material.

Conflicts of interest

The authors declare that they have no conflict of interest.

Acknowledgements

The present work was supported financially by the Natural Science Foundation of Hebei Province (Grant E2018502054). This work was also supported by the Fundamental Research Funds for the Central Universities (Grant 2017MS141).

Notes and references

[a] *Department of Environmental Science and Engineering, North China Electric Power University, Baoding, 071003, China. Tel: +86 0312 7525228, E-mail: duancw@ncepu.edu.cn.*

[b] *School of Materials Science and Engineering, Harbin Institute of Technology, Harbin, 150001, China. Tel: +86 0451 86418613.*

[c] *School of Information Science and Engineering, Hebei University of Science and Technology, Shijiazhuang, 050018, China.*

1 W. Grochala and P. P. Edwards, *Chem. Rev.*, 2004, **104**, 1283-1316.

View Article Online
DOI: 10.1039/C8TA00533H

2 S. I. Orimo, Y. Nakamori, J. R. Eliseo, A. Züttel and C. M. Jensen, *Chem. Rev.,* 2007, **107**, 4111-4132.
3 G. C. Sinke, L. C. Walker and F. L. Oetting, *J. Chem. Phys.*, 1967, **47**, 2759-2761.
4 C. Wolverton, V. Ozolinš and M. Asta, *Phys. Rev. B*, 2004, **69**, 144109.
5 S. Gupta, T. Kobayashi, I. Z. Hlova, J. F. Goldston, M. Pruski and V. K. Pecharsky, *Green Chem.*, 2014, **16**, 4378-4388.
6 J. Graetz, *Chem. Soc. Rev.*, 2009, **38**, 73-82.
7 Y. Nakagawa, S. Isobe, Y. Wang, N. Hashimoto, S. Ohnuki, L. Zeng, L. Shusheng, I. Takayuki and Y. Kojima, *J. Alloy. Compd.*, 2013, **580**, S163-S166.
8 J. Graetz and J. J. Reilly, *J. Phys. Chem. B*, 2005, **109**, 22181-22185.
9 J. Yang, P. R. Beaumont and T. D. Humphries, *Energies*, 2015, **8**, 9107-9116.
10 T. Bazyn, R. Eyer, H. Krier and N. Glumac, *J. Propul. Power*, 2004, **20**, 427-431.
11 L. T. DeLuca, L. Rossettini and C. Kappenstein, *AIAA Paper*, 2009, **4874**, 2009.
12 J. W. Turley and H. W. Rinn, *Inorg. Chem.*, 1969, **8**, 18-22.
13 X. Ke, A. Kuwabara and I. Tanaka, *Phys. Rev. B*, 2005, **71**, 184107.
14 H. W. Brinks, A. Istad-Lem and B. C. Hauback, *J. Phys. Chemistry. B*, 2006, **110**, 25833-25837.
15 H. W. Brinks, W. Langley, C. M. Jensen, J. Graetz, J. J. Reilly and B. C. Hauback, *J. Alloy. Compd.*, 2007, **433**, 180-183.
16 V. A. Yartys, R. V. Denys, J. P. Maehlen, Ch. Frommen, M. Fichtner, B. M. Bulychev and H. Emerich, *Inorg. Chem.*, 2007, **46**, 1051-1055.
17 F. M. Brower, N. E. Matzek, P. F. Reigler, H. W. Rinn, C. B. Roberts, D. L. Schmidt, J. A. Snover and K. Terada, *J. Am. Chem. Soc.*, 1976, **98**, 2450-2453.
18 B. M. Bulychev, V. N. Verbetskii and A. I. Sizov, *Russ. Chem. Bulletin*, 2007, **56**, 1305-1312.
19 B. M. Bulychev, V. N. Verbetskii and P. A. Storozhenko, *Russ. J. Inorg. Chem.*, 2008, **53**, 1000-1005.
20 Y. Kim, E.-K. Lee, J.-H. Shim, Y. W. Cho and K. B. Yoon, *J. Alloy. Compd.,* 2006, **422**, 283-287.
21 K. T. Møller, J. B. Grinderslev and T. R. Jensen, *J. Alloy. Compd.*, 2017, **720**, 497-501.
22 V. Birke, J. Mattik and D. Runne, *J. Mater. Sci.*, 2004, **39**, 5111-5116.
23 G. T. Tigineh, Y. S. Wen and L. K. Liu, *Tetrahedron*, 2015, **71**, 170-175.
24 B. I. Park, S. Yu and Y. Hwang, *J. Mater. Chem. A*, 2015, **3**, 2265-2270.
25 S. Sartori, A. Istad-Lem, H. W. Brinks and B. C. Hauback, *Int. J. Hydrogen Energ.*, 2009, **34**, 6350-6356.
26 M. Paskevicius, D. Sheppard and C. Buckley, *J. Alloy. Compd.*, 2009, **487**, 370-376.
27 L. V. Dinh, D. A. Knight and M. Paskevicius, *Appl. Phys. A*, 2012, **107**, 173-181.
28 J. R. A. Fernandez, F. Aguey-Zinsou and M. Elsaesser, *Int. J. Hydrogen Energ.*, 2007, **32**, 1033-1040.
29 F. L. Zhang, M. Zhu and C. Y. Wang, *Int. J. Refract. Met. H. Mat.*, 2008, **26**, 329-333.
30 S. Sartori, S. M. Opalka and O. M. Løvvik, *J. Mat. Chem.*, 2008, **18**, 2361-2370.
31 I. Z. Hlova, S. Gupta and J. F. Goldston, *Faraday Discuss.*, 2014, **170**, 137-153.
32 M. Ishikawa, T. Sugimoto and M. Kikuta, *J. Power Sources*, 2006, **162**, 658-662.
33 H. Matsumoto, H. Sakaebe and K. Tatsumi, *J. Power Sources*, 2006, **160**, 1308-1313.
34 N. J. K. Rantonen, T. Toyabe and T. Maekawa, *Carbon*, 2008, **46**, 1225-1231.
35 A. Zare, A. Parhami and A. R. Moosavi-Zare, *Can. J. Chem.*, 2008, **87**, 416-421.
36 L. X. Hu, H. Wang and X. Wang, *J. Alloy. Compd.*, 2012, **513**, 343-346.
37 C. W. Duan, L. X. Hu and Y. Sun, *RSC Adv.*, 2015, **5**, 17104-17108.
38 C. W. Duan, L. X. Hu and D. Xue, *Green Chem.*, 2015, **17**, 3466-3474.
39 C. W. Duan, L. X. Hu and Y. Sun, *Phys. Chem. Chem. Phys.*, 2015, **17**, 22152-22159.
40 C. W. Duan, L. X. Hu and Y. Sun, *Dalton Trans.*, 2015, **44**, 16251-16255.
41 L. He, S. Wang and Z. Li, *Rare Metals*, 2011, **30**, 55-58.
42 L. Zaluski, A. Zaluska and J. O. Ström-Olsen, *J. Alloy. Compd.*, 1999, **290**, 71-78.
43 G. Mairesse, P. Barbier and J. P. Wignacourt, *Acta. Crystallog. B*, 1979, **35**, 1573-1580.
44 T. D. Humphries, K. T. Munroe, T. M. DeWinter, C. M. Jensen and G. S. McGrady, *Int. J. Hydrogen Energ.*, 2013, **38**, 4577-4586.
45 S. J. Hwang , R. C. Bowman and J. Graetz, *J. Alloy. Compd.*, 2007, **446**, 290-295.
46 S. D. Beattie, T. Humphries and L. Weaver, *Chem. Commun.*, 2008, **37**, 4448-4450.
47 J. Graetz and J. J. Reilly, *J. Alloy. Compd.*, 2006, **424**, 262-265.
48 R. Chen, C. L. Duan and X. Liu, *J. Vac. Sci. Technol. A*, 2017, **35**, 03E111.
49 J. Graetz, J. J. Reilly and J. G. Kulleck, *J. Alloy. Compd.*, 2007, **446**, 271-275.
50 H. Liu, X. Wang, Y. Liu, Z. Dong, S. Li, H. Ge and M. Yan, *The J. Phys. Chemistry. C*, 2014, **118**, 18908-18916.
51 H. Liu, X. Wang, Y. Liu, Z. Dong, H. Ge, S. Li and M. Yan, *J. Phys. Chemistry. C*, 2013, **118**, 37-45.
52 H. Liu, X. Wang, H. Zhou, S. Gao, H. Ge, S. Li and M. Yan, *Int. J. Hydrogen Energ.,* 2016, **41**, 22118-22127.
53 J. Graetz, J. J. Reilly, V. A. Yartys, J. P. Maehlen, B. M. Bulychev, V. E. Antonov, B. P. Tarasov and I. E. Gabis, *J. Alloy. Compd.*, 2011, **509**, S517-S528.
54 G. Sandrock, J. Reilly, J. Graetz, w.-m. Zhou, J. Johnson and J. Wegrzyn, *Appl. Phys. A*, 2005, **80**, 687-690.
55 H. Liu, X. Wang, Z. Dong, G. Cao, Y. Liu, L. Chen and M. Yan, *Int. J. Hydrogen Energ.*, 2013, **38**, 10851-10856.
56 H. Liu, X. Wang, Y. Liu, Z. Dong, G. Cao, S. Li and M. Yan, *J. Mater. Chem. A*, 2013, **1**, 12527-12535.
57 P. J. Herley and O. Christofferson, *J. Phys. Chem.* 1981, **85**, 1887-1892.
58 Z. Cao, L. Ouyang, H. Wang, J. Liu, M. Felderhoff and M. Zhu, *J. Mater. Chem. A*, 2017, **5**, 6042-6046.
59 I. Gabis, M. Dobrotvorskiy and E. Evard, *J. Alloy. Compd.*, 2011, **509**, S671-S674.

View Article Online
DOI: 10.1039/C8TA00533H

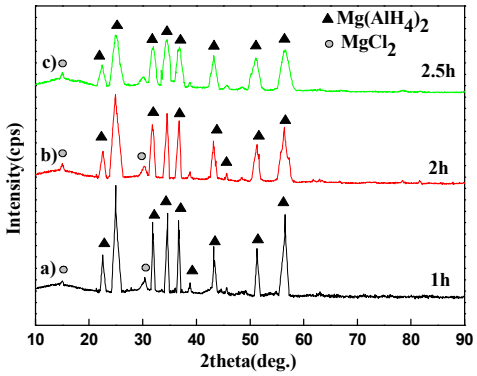

Fig. 1 XRD patterns of as-milled $MgH_2/AlCl_3$ powders milled with BPR of 20:1 at 200 rpm for different times: a) 1h, b)2h, c)2.5h

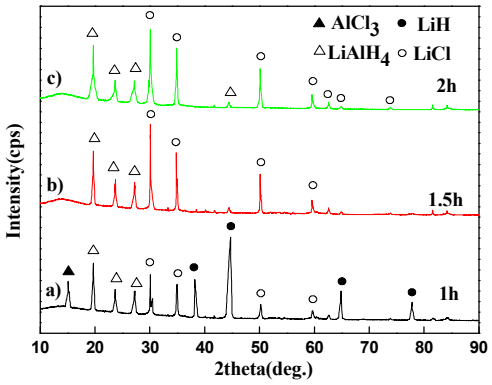

Fig. 2 XRD patterns of as-milled $LiH/AlCl_3$ powders milled with BPR of 20:1 at 200 rpm for different times: a) 1h, b)2h, c)2.5h

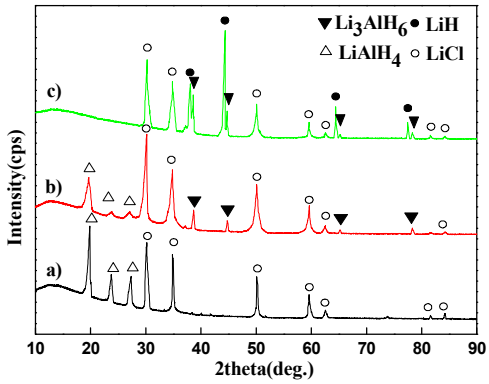

Fig. 3 The XRD patterns of the as-milled samples with $LiH:AlCl_3$ starting ratios of a) 4:1, b) 6:1 and c) 9:1 after ball-milling for 1h with a milling speed of 200 rpm and a BPR of 40.

View Article Online
DOI: 10.1039/C8TA00533H

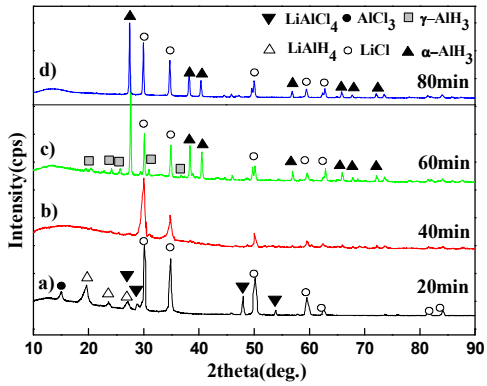

Fig. 4 XRD patterns of samples obtained from the 4:1 reaction of LiH and $AlCl_3$ ($LiAlH_4$, LiCl at τBM = 60 min) after ball-milling for the various times: a) 20min, b)40min, c)60min and d)80min, with a milling speed of 200 rpm and BPR of 40.

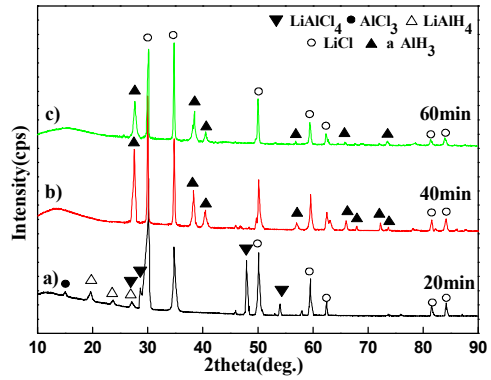

Fig. 5 XRD patterns of samples obtained from the 4:1 reaction of LiH and $AlCl_3$ ($LiAlH_4$, LiCl at τBM = 60 min) after ball-milling for the various times: a) 20min, b)40min and c)60min, with a milling speed of 200 rpm and BPR of 60.

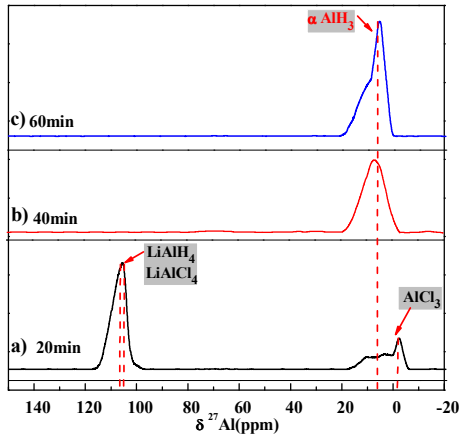

Fig. 6 Solid-state ^{27}Al NMR spectra of obtained samples after ball-milling for the 20, 40, 60min with a milling speed of 200 rpm and a b:p of 60. Noted that the obtained samples were synthesized from the 4:1 reaction of LiH and $AlCl_3$ milling for 60 min.

View Article Online
DOI: 10.1039/C8TA00533H

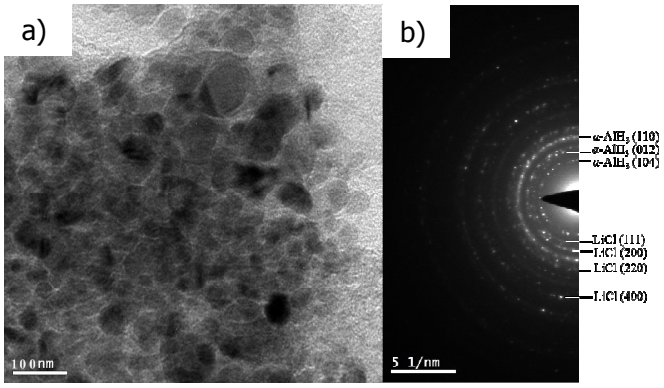

Fig. 7 TEM images as well as electron diffraction patterns of α-AlH_3 composite milled with 60:1 ratios for 60min.

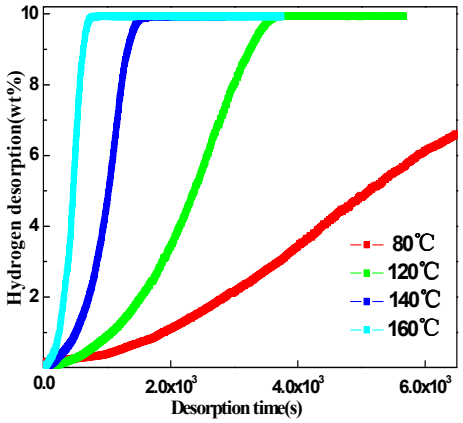

Fig. 8 The dehydriding curves of α-AlH_3/LiCl composite at different temperatures. Hydrogen content is calculated by percentage of the calculated non-salt portion of the sample.

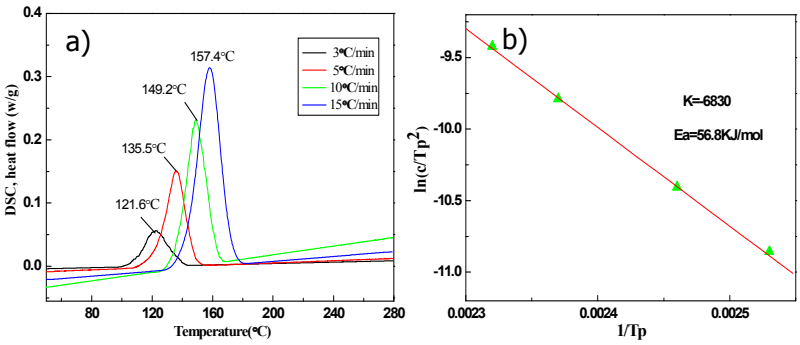

Fig. 9 (a) DSC curves of α-AlH_3/LiCl composite in temperature ranges from 50 to 280 °C; (b) The apparent energy for the decomposition obtained from DSC measurements.

View Article Online
DOI: 10.1039/C8TA00533H

Basic reaction in the process

$$4LiH + AlCl_3 \rightarrow LiAlH_4 + 3LiCl$$

$$3LiAlH_4 + AlCl_3 \rightarrow 3LiCl + 4\alpha\text{-}AlH_3$$